Third International Symposium on Marine Propulsors
smp'13, Launceston, Tasmania, Australia, May 2013

Model and full scale CFD analysis of propeller boss cap fins (PBCF)

Takafumi Kawamura[1], Kazuyuki Ouchi[2], Susumu Takeuchi[3]

[1]Computational Fluid Dynamics Consulting Inc., Japan
[2]Faculty of Systems Innovation, School of Engineering, the University of Tokyo, Japan
[3]PBCF department, MOL Techno-Trade, Ltd., Japan

ABSTRACT

CFD analyses of PBCF (Propeller Boss Cap Fins) were carried out for two different propellers at model and full scale Reynolds numbers with two different inflow conditions. Computations corresponding to the reverse POT experiment were confirmed to be in a good agreement with the measurement. The results of computations at different conditions have shown that increased Reynolds number and presence of hull wake both positively influence the effects of PBCF. Due to the combined effect of the Reynolds number and the wake, the gain in the propeller efficiency at the full scale condition was found to be significantly larger than that at the model test condition. The detailed investigation of the results suggested that the fin drag becomes smaller and the reduction of the boss drag becomes larger at the full scale condition. However, the predicted gain is still smaller than the values reported in the sea trial and logbook analysis. The remaining gap may be attributed to the difference in the estimated and actual wake distribution or to other factors such as interactions with hull and rudder, surface roughness, unsteadiness and hub vortex cavitation.

Keywords

PBCF, CFD, full scale Reynolds number

Symbols

D	propeller diameter
J	advance coefficient
n	rotation speed
K_T	thrust coefficient $K_T = \dfrac{\text{Thrust}}{\rho n^2 D^4}$
K_Q	torque coefficient $K_Q = \dfrac{\text{Torque}}{\rho n^2 D^5}$
R_{nD}	propeller Reynolds number $R_{nD} = \dfrac{nD^2}{\nu}$
C_{pn}	pressure coefficient $C_{pn} = \dfrac{\text{Pressure}}{\rho n^2 D^2}$
η	propeller efficiency $\eta = \dfrac{J \cdot K_T}{2\pi K_Q}$
V_0	velocity of the uniform flow
ρ	density
ν	kinematic viscosity

1 INTRODUCTION

The PBCF is known to be one of the most successful energy-saving devices for ships. More than 2,000 sets have been sold since its first introduction in 1987. As shown in Figure 1, the PBCF consists of small fins attached on the boss cap fixed to the propeller and is designed to recover energy from the propeller hub vortex. The number of fins is the same as that of the propeller blades.

The research and development of PBCF were originally carried out by Ouchi et al. (1988, 1989, 1992) They confirmed that thrust increases and torque decreases, thus the efficiency increases with the introduction of PBCF. The measured increase of the efficiency in their model experiments was from 1 to 2%. The early work by Ouchi et al. and activities of other groups on various boss cap designs are reviewed by Atler and Patience (1998) in detail. Recently, results of more systematic experiments are published by Nojiri et al. (2011) for four, five and six-

Figure 1 Example of PBCF (Propeller Boss Cap Fins) installed on a ship

bladed propellers. The measured increase of the propeller efficiency was from 1 to 1.5%. More recently, Hansen et al. (2011) reported a model and full scale evaluation of PBCF fitted to an Aframax tanker. In their study, the measured increase of the efficiency in the model test was also about 1%. The results of the model tests by those different groups are consistent, and it is suggested that the increase of the efficiency in the model experiment is approximately from 1 to 2%.

On the other hand, Ouchi (1992) reported the results of full scale analyses for 12 different vessels, in which the average energy-saving effect of PBCF was 5.4%. Hansen et al. (2011) reported that the analysis of the sea trials showed 3.5% and 4% reduction in shaft horsepower in ballast and in load condition, respectively. Nojiri et al. (2011) also showed the results of full scale analyses for 16 different vessels, in which the energy-saving effect ranges from 2 to 10% with the average being approximately 5%. Those facts suggest that the energy-saving effect of PBCF is larger in full scale than in model tests, although the uncertainty in full scale analysis is generally larger. The presence of substantial scale effect was also suggested by Ouchi et al. (1989, 1992), Nojiri et al. (2011), and in the report of ITTC specialist committee (1999).

The reason for the difference is currently unknown. However, it is presumed that the differences in the Reynolds number and in the flow condition have significant influence. The typical diameter of the model propeller is 250mm, and the Reynolds number is on the order of 10^5, while it is usually on the order of 10^7 in full scale. The inflow into the propeller has strong variation in actual operation because of the presence of ship wake, but the inflow has much less variation in the experiments (Ouch et al. 1988).

The purpose of this paper is to investigate the influence of the Reynolds number and the inflow condition on the energy-saving effect of PBCF by CFD. Firstly, the reliability of CFD methods is examined carefully through comparisons with the experiments. Then simulations at model and full scale Reynolds numbers are carried out for two different propellers. Based on the numerical results the influences of the Reynolds number and the inflow condition on the effects of PBCF are discussed.

2 FLOW MODEL AND NUMERICAL METHODS

Figure 2 shows the schematic sketch of the reverse and normal POT experiments (Ouch et al. 1988). The flow direction in the reverse POT is opposite from that in the normal POT. Ouchi et al. (1988) found that the effect of PBCF can not be measured in the normal POT setup because the hub vortex is missing. Therefore, the development of PBCF has been carried out using the reverse POT method. The setup of the CFD simulation was also made after the reverse POT experiments. Figure 3 shows the computational domain with the definition of the coordinate axes. By using a periodic boundary condition, only one set of blade and fin is computed. Figure 4 provides closer view of the computational domain around a set of blade and fin. The origin of the coordinate system is located on the rotation axis at the position of the propeller generator line. The inflow and outflow boundaries are located at and respectively. The radial size of the domain is set to .

The numerical methods used in this study follow the previous work by the first author (Kawamura & Omori 2008). The rotating coordinate system fixed to the propeller is adopted, and steady state is assumed in the computation. The governing equations are the Reynolds Averaged Navier-Stokes equations and the continuity equation for incompressible Newtonian fluid. A commercial CFD software Fluent version 6.3 was used as the solver. Fluent is an unstructured mesh based finite volume solver, and has been successfully applied to flow around marine propellers (Kawamura et al. 2004, Rhee et al. 2005, Kawamura 2011). The k-w-SST model was used for turbulence modeling, and QUICK scheme was selected as the discretization scheme. The steady state solution was obtained by SIMPLE algorithm.

Figure 5 shows an example of the computational mesh on the blade, fin and boss surfaces. Layers of prismatic cells are placed on the blade and fin surfaces for resolving the boundary layer. Mesh generation was carried out carefully so that the Reynolds number effect is correctly accounted for. The height of the cell adjacent to the blade surface is kept at unity in the viscous unit (Kawamura & Omori 2008). Other meshing parameters are chosen following the previous studies (Kawamura & Omori 2008, Kawamura 2011), so that the grid dependency is sufficiently small for the purpose of the simulation. The total number of computational cells is about 1.3 million for simulation at full scale Reynolds number.

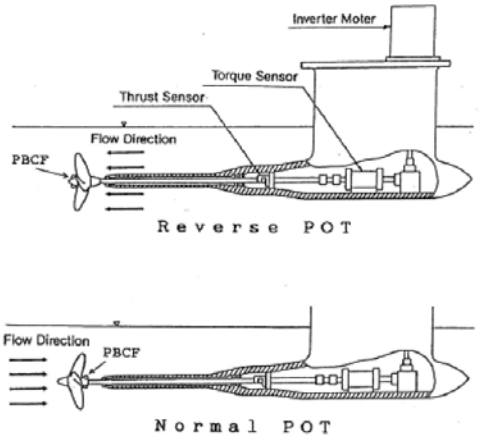

Figure 2 Arrangement of reverse POT and normal POT

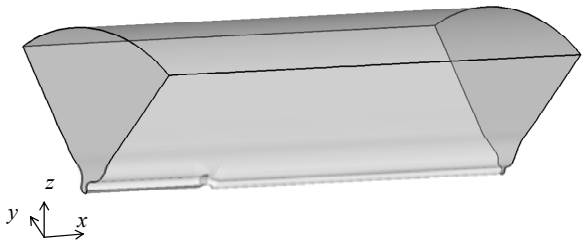

Figure 3 Computational domain

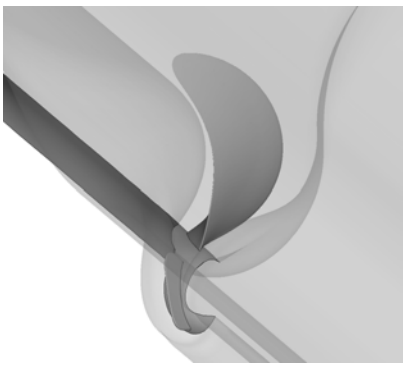

Figure 4 Computational domain around one blade and fin

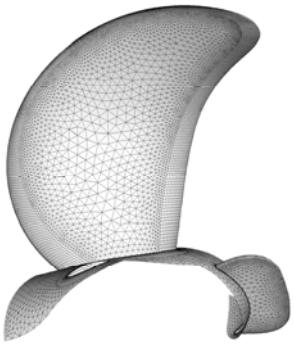

Figure 5 Computational mesh on the blade, fin and boss surfaces

3 CONDITION OF COMPUTATION

Computations were performed for two different propellers both at model and full scale Reynolds numbers. Table 1 shows the principal particulars of the two propellers, and Figure 6 shows perspective views of the propeller models. Propeller-A is a 5 bladed highly skewed propeller made for a 44,800 gross tonnage PCC, Mercury Ace for which the energy-saving effect of the PBCF is estimated to be about 4% in the sea trial (Ouch et al. 1989). Propeller-B is a 5 bladed conventional propeller for a 98,587 gross tonnage bulk carrier, Asakasan-maru. According to the logbook analysis data, the effect of the PBCF is estimated to be also about 4%. The reverse POT experiment for Propeller-A was carried out in MARIN (Maritime Research Institute Netherlands) by Ouchi et al. (1989), while that for Propeller-B was carried out in the West Japan Fluid Engineering Laboratory using the apparatus and procedure of the model tests are described more in detail by Ouchi et al. (1988).

Influence of the inflow condition was investigated by imposing two different axial wake distributions at the inlet boundary. In general, wake distributions have variations both in the radial and circumferential directions. While the circumferential variation has significant influence on cavitation performance, the radial variation has dominant effect on the propulsion performance (Yamasaki 1989). Therefore, only the radial variation is taken into account in this study. Wake-A simulates the wake of the reverse POT apparatus measured by Ouchi et al. (1988), while wake-B simulates that of the full scale ship.

Table 1 Principal particulars of the propellers

	Propeller-A		Propeller-B	
Name of ship	Mercury Ace		Asakasan-maru	
Type of ship	PCC		Bulk Carrier	
Pitch ratio	0.89		0.8073	
E. A. R.	0.6		0.58	
Boss ratio	0.1888		0.1683	
Blade section	MAU		MAU	
Blade number	5		5	
	Model	Ship	Model	Ship
Diameter	200 (mm)	5.35 (m)	250 (mm)	7.9 (m)
Revolution	7 (rps)	116 (rpm)	8.02 (rps)	80.8 (rpm)

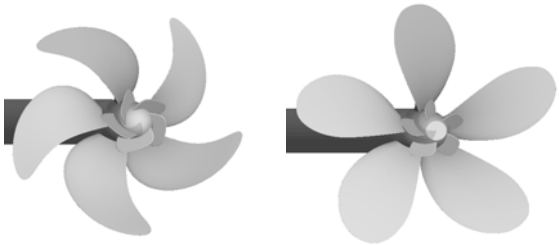

(a) Propeller-A (b) Propeller-B

Figure 6 Models of propellers with fins

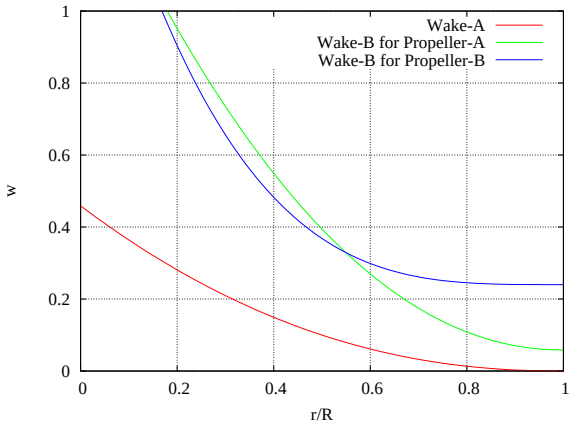

Figure 7 Wake distribution used for computation

The wake distributions are circumferentially averaged and approximated as Figure 7. Because wake-B depends on the wake measurement of the ship models, different distributions are used for Propeller-A and B. The inflow velocity V is given as,

$$V = (1 - w(r))V_0 \quad (1)$$

where V_0 is the velocity of the uniform flow, and $w(r)$ is the wake distribution shown in Figure 7. It should be noted that the boundary layer around the shaft is missing in wake-A. This is because the resolution in the measurement was not sufficient to resolve the thin boundary layer. In this study, the presence of the thin boundary layer is not included in wake-A. The validity of the inflow condition is investigated through the comparison of the propeller performance between the experiment and computation.

4 RESULTS

4.1 Results at Model Scale Reynolds Number

Comparison of the measured and computed propeller characteristics without PBCF in the reverse POT at model scale Reynolds number is shown in Figure 8 and 9 for Propeller-A and B respectively. The inflow velocity distribution of wake-A was used in the computation. The Reynolds number based on the diameter is 2.1×10^5 for Propeller-A, and 2.7×10^5 for Propeller-B. The advance coefficient J is defined as

$$J=\frac{V_0}{nD} \tag{2}$$

The value of J in the computation is calculated by so-called thrust identity method. Therefore, the measured and computed values of the thrust coefficient in Figures 8 and 9 are exactly the same. The overall agreement between the measurement and computation is good except that computation overestimates the torque coefficient. However, the difference is consistent and about 2% for both propellers. The overestimation of torque in computation is also reported in the previous studies (Kawamura & Omori 2008, Rhee et al. 2005, Kawamura 2011). The reason is probably the presence of laminar region in the boundary layer over the blade surface in the experiment (Kawamura & Omori 2008).

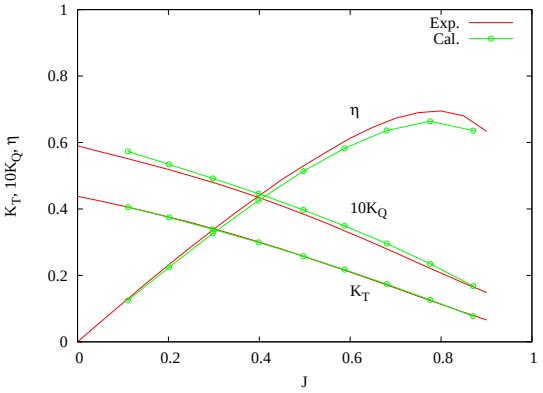

Figure 8 Comparison of the measured and computed characteristics of Propeller-A in wake-A without PBCF at model scale Reynolds number.

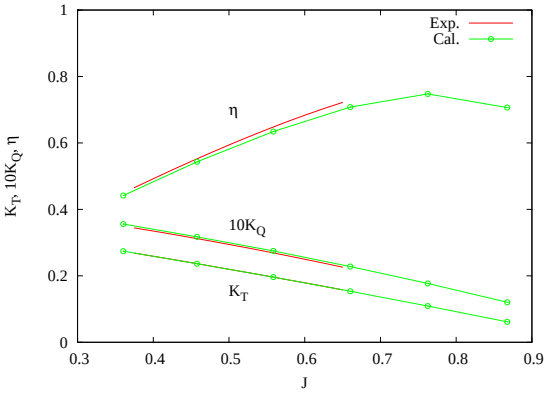

Figure 9 Comparison of the measured and computed characteristics of Propeller-B in wake-A without PBCF at model scale Reynolds number

Figure 10 shows the distribution of the pressure coefficient on the blades, fins and boss surfaces at J=0.7 for Propeller-A. From this figure, it is observed that the angle of attack of the fins is opposite from that of the main blades. That is, pressure distribution on the fins generates negative thrust and torque.

The effect of the PBCF was evaluated in terms of the relative change of the thrust and torque coefficients and the propeller efficiency. For example, the relative change of the thrust coefficient is defined as

$$\frac{\Delta K_T}{K_T}=\frac{K_T'-K_T}{K_T} \tag{3}$$

in which K_T is the thrust coefficient without PBCF, and K_T' is that with PBCF. The relative change of the torque coefficient K_Q and the propeller efficiency η are defined in the same manner.

Figure 11 shows the measured and computed effect of PBCF for Propeller-A in the reverse POT at model scale Reynolds number. The measurement shows that the thrust coefficient increases by about 1%, and the torque coefficient decreases by about 1%. As a result, the propeller efficiency increases by about 2%. The results of the computation are consistent with the measurement. Based on this comparison, it is considered that the present setup of the computation including the inflow condition is reasonable for discussing the effect of PBCF. The sources of remaining difference between the measurement and computation probably include the uncertainties in the measurement. Since the magnitude of the changes in K_T and K_Q is on the order of 1%, the measurement is very sensitive. Although the quantitative uncertainty assessment was not carried out in the experimental studies (Ouchi et al. 1988, 1989), it must be assumed some error is included in the measurement.

Figure 12 shows the same comparison for Propeller-B. The measured relative increase of the propeller efficiency is from about 1.5 to 2 %, which is the result of the increase in K_T and decrease in K_Q. The computation also predicted increase in K_T, decrease in K_Q and about 1.5% increase in η.

While only the net thrust and torque can be measured in the experiment, they can be decomposed in the computation. For example, the thrust coefficient can be decomposed as

$$K_T=K_{T\,\mathrm{BLADE}}+K_{T\,\mathrm{BOSS}}+K_{T\,\mathrm{FIN}} \tag{4}$$

where $K_{T\,\mathrm{BLADE}}$, $K_{T\,\mathrm{BOSS}}$ and $K_{T\,\mathrm{FIN}}$ are the contributions to the thrust coefficient of the blade, boss and fin, respectively. The torque coefficient can be decomposed in the same manner. The relative change of the thrust coefficient due to PBCF can be also decomposed as

$$\frac{\Delta K_T}{K_T}=\frac{\Delta K_{T\,\mathrm{BLADE}}}{K_T}+\frac{\Delta K_{T\,\mathrm{BOSS}}}{K_T}+\frac{\Delta K_{T\,\mathrm{FIN}}}{K_T} \tag{5}$$

in which $\Delta K_{T\,\mathrm{BLADE}}$ and $\Delta K_{T\,\mathrm{BOSS}}$ are the change of

$K_{T\,BLADE}$ and $K_{T\,BOSS}$ by the introduction of PBCF, while $\Delta K_{T\,FIN}$ is the thrust coefficient of the fins. The relative change of the torque coefficient can be decomposed in the same manner, but $\Delta K_{Q\,BOSS}$ is ignored since it is two orders of magnitude smaller than the other components.

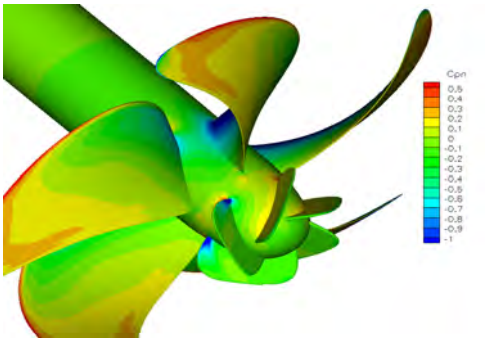

Figure 10 Distribution of the pressure coefficient C_{pn} on the blades, fins and boss surface of Propeller-A at J=0.7 in wake-A at model scale Reynolds number

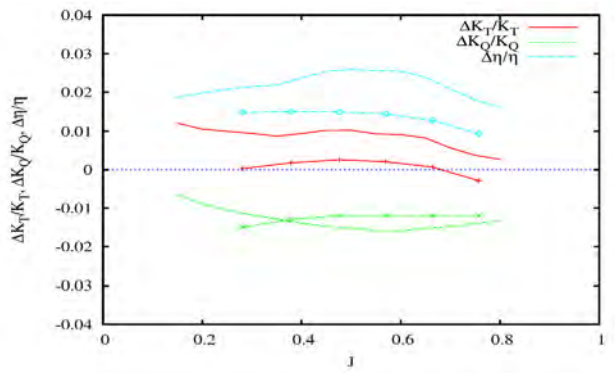

Figure 11 Comparison of the measured (lines without symbol) and computed (lines with symbols) effect of PBCF for Propeller-A in wake-A at model scale Reynolds number

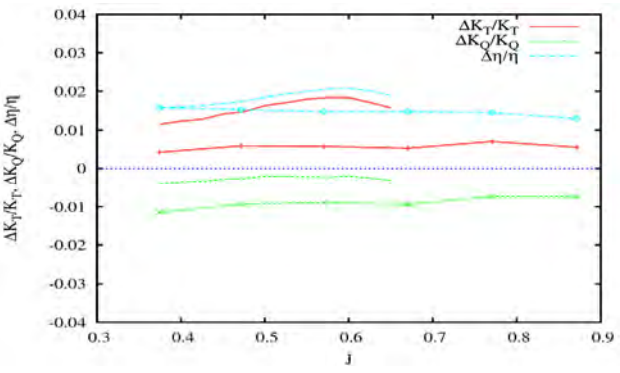

Figure 12 Comparison of the measured (lines without symbol) and computed (lines with symbols) effect of PBCF for Propeller-B in wake-A at model scale Reynolds number

Figure 13 and 14 show the components of the effect of PBCF for Propeller-A and Propeller-B, respectively. For both propellers, $\Delta K_{T\,BOSS}$ is always positive, and its magnitude is about 2% of the total thrust, while $\Delta K_{T\,FIN}$ is negative and its magnitude is similar to that of $\Delta K_{T\,BOSS}$. The torque coefficient of the fins $\Delta K_{Q\,FIN}$ is always negative and its magnitude is about 1% of the total torque coefficient. The magnitude of $\Delta K_{T\,BLADE}$ and $\Delta K_{Q\,BLADE}$ is smaller than the other three components. However, $\Delta K_{T\,BLADE}$ is consistently larger than $\Delta K_{Q\,BLADE}$. This means that the change in the thrust and torque of the blade also contributes to the increase of the propeller efficiency. As the advance coefficient J increases, the relative magnitude of $\Delta K_{T\,FIN}$ and $\Delta K_{Q\,FIN}$ increases because the angle of the attack of the fins to the incoming flow is increased. At the same time, $\Delta K_{T\,BLADE}$ and $\Delta K_{Q\,BLADE}$ also increase probably because of decreased axial velocity due to the increased drag of fins.

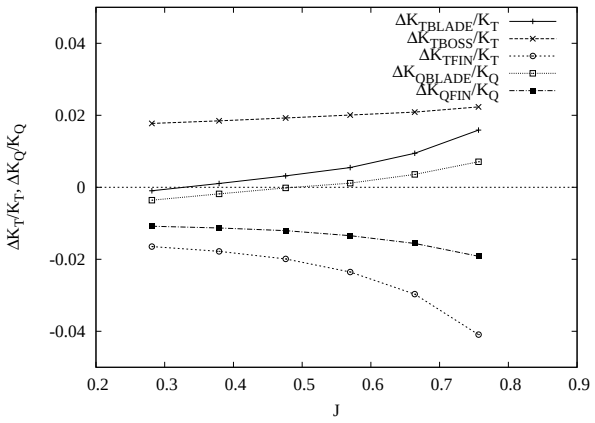

Figure 13 Components of the effect of PBCF for Propeller-A in wake-A at model scale Reynolds number

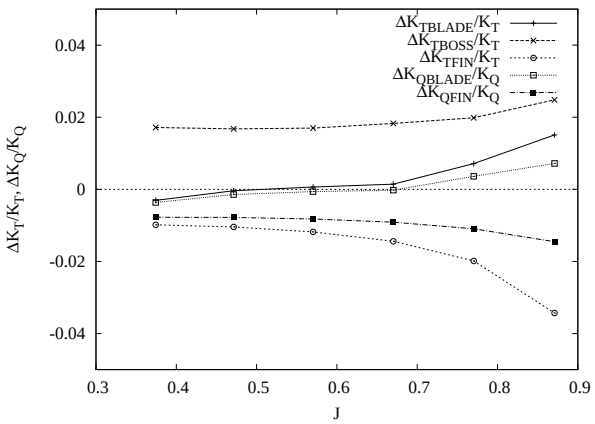

Figure 14 Components of the effect of PBCF for Propeller-B in wake-A at model scale Reynolds number

The effect of the fins in wake-B is compared with that in wake-A in Figure 15 and 16 for Propeller-A and Propeller-B, respectively. Increase in the propeller efficiency is slightly larger in wake-B than in wake-A for both propellers. For Propeller-A, the increase of the thrust coefficient contributes to the increase of the efficiency, while both increase of the thrust and increase of the negative torque contribute to the increase of the efficiency for Propeller-B. It is noticed that the increase of the propeller efficiency due to PBCF is almost independent of the blade loading condition for both Propeller-A and B regardless of the inflow condition. This fact suggests that the optimum fin design depends mainly on the blade configuration than the loading condition.

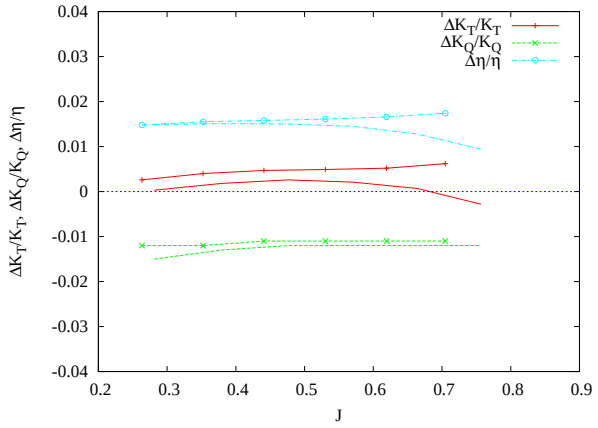

Figure 15 Comparison of the effect of PBCF for Propeller-A in wake-A (lines without symbols) and in wake-B (lines with symbols) at model scale Reynolds number

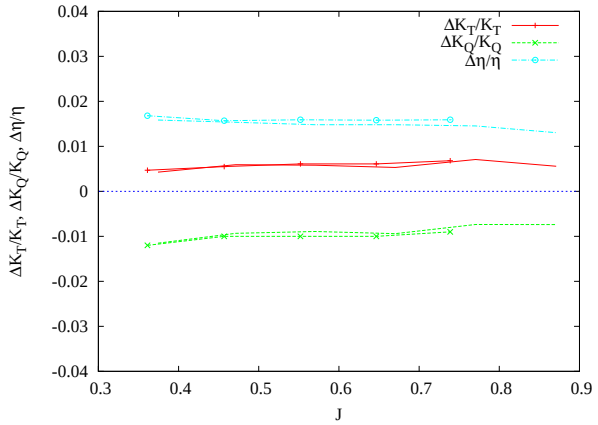

Figure 16 Comparison of the effect of PBCF for Propeller-B in wake-A (lines without symbols) and in wake-B (lines with symbols) at model scale Reynolds number

4.2 Results at Full Scale Reynolds Number

The effect of PBCF in wake-B at model and full scale Reynolds numbers are compared in Figure 17 and 18 for Propeller-A and Propeller-B, respectively. It is noted that the increase of the propeller efficiency is significantly larger at the full scale Reynolds number than at the model scale model Reynolds number for both propellers. This is mainly due to that the increase of thrust is larger at full scale Reynolds number.

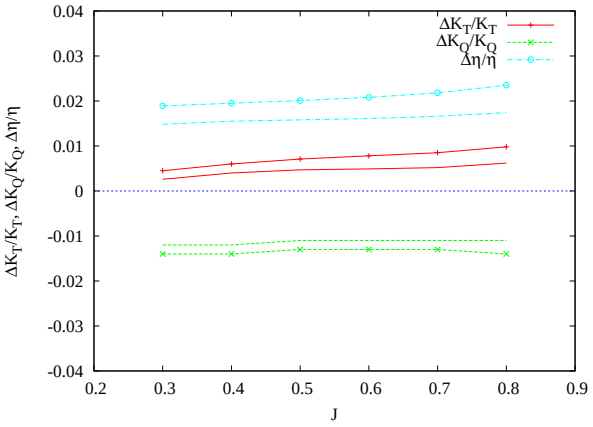

Figure 17 Comparison of the effect of PBCF for Propeller-A in wake-B at model scale (lines without symbols) and at full scale (lines with symbols) Reynolds numbers

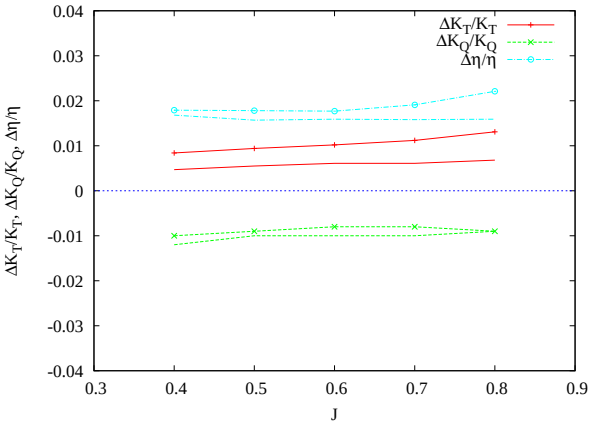

Figure 18 Comparison of the effect of PBCF for Propeller-B in wake-B at model scale (lines without symbols) and at full scale (lines with symbols) Reynolds numbers

5 DISCUSSION

Computations at model scale and full scale Reynolds numbers with different inflow conditions have shown that higher Reynolds number and the presence of wake of the hull positively influence the effect of PBCF. Tables 3 and 4 show the components of the effect of PBCF at J=0.7 at four different combinations of Reynolds number and inflow conditions. In Tables 3 and 4, the increase of η

Table 3 Comparison of the components of the effect of PBCF for Propeller-A at J=0.7

	$\Delta K_{T\,BLADE}$	$\Delta K_{T\,BOSS}$	$\Delta K_{T\,FIN}$	$\Delta K_{Q\,BLADE}$	$\Delta K_{Q\,FIN}$	$\Delta\eta$
Model scale in wake-A	0.55%	2.01%	-2.35%	0.11%	-1.34%	1.48%
Model scale in wake-B	0.52%	2.29%	-2.30%	0.12%	-1.25%	1.73%
Full scale in wake-A	0.48%	2.23%	-2.23%	0.11%	-1.52%	2.02%
Full scale in wake-B	0.41%	2.50%	-2.08%	0.07%	-1.38%	2.32%

Table 4 Comparison of the components of the effect of PBCF for Propeller-B at J=0.7

	$\Delta K_{T\,BLADE}$	$\Delta K_{T\,BOSS}$	$\Delta K_{T\,FIN}$	$\Delta K_{Q\,BLADE}$	$\Delta K_{Q\,FIN}$	$\Delta\eta$
Model scale in wake-A	0.70%	1.95%	-1.95%	0.36%	-1.09%	1.49%
Model scale in wake-B	0.22%	1.93%	-1.55%	0.05%	-0.94%	1.56%
Full scale in wake-A	0.76%	2.11%	-1.83%	0.50%	-1.24%	1.87%
Full scale in wake-B	0.31%	2.12%	-1.32%	0.15%	-0.95%	2.05%

was calculated at the same loading condition $\left(K_T / J^2\right)$ by linear interpolation. The increase of η is larger in wake-B than in wake-A in all cases, namely for both propellers at model and full scale Reynolds numbers. This is partially due to that the drag of fins $\Delta K_{T\,FIN}$ is smaller in wake-B than in wake-A, because the axial velocity around the fins is smaller.

The increase of η is also larger at the full scale Reynolds number than at the model scale Reynolds number in all cases, namely for both propellers in wake-A and in wake-B. This is due to that $\Delta K_{T\,FIN}$ is smaller, and $\Delta K_{Q\,FIN}$ is larger at the full scale Reynolds number than at the model scale Reynolds number. That is, the efficiency of fins is higher at the full scale Reynolds number. The larger decrease of the boss drag $\Delta K_{T\,BOSS}$ also contributes to the larger increase in the efficiency.

Figure 19 and 20 compare the components of the effect of PBCF in wake-A at model scale Reynolds number, which corresponds to the reverse POT experiment, and in wake-B at full scale Reynolds number, which is close to actual trial or voyage condition. The left hand side and right hand side compare the negative and positive effects of PBCF, respectively. The fin drag $\Delta K_{T\,FIN}$ is smaller in wake-B at full scale Reynolds number. Since the $\Delta K_{T\,BLADE}$ and $\Delta K_{Q\,BLADE}$ are related with $\Delta K_{T\,FIN}$, they are also smaller in wake-B at full scale Reynolds number. It is also found that the reduction of the boss drag $\Delta K_{T\,BOSS}$ is significantly larger in wake-B at full scale Reynolds number.

Due to the combined effect of the wake and the Reynolds number, the gain in the propeller efficiency $\Delta\eta/\eta$ for Propeller-A is increased from 1.48% at the condition corresponding to the reverse POT experiment to 2.32% at the condition close to the trial or voyage condition, and that for Propeller-B is increased from 1.49% to 2.05%. Roughly speaking, about two thirds of the increase can be attributed to the Reynolds number effect as shown in Table 3 and 4.

The gain in the efficiency at the condition corresponding to the reverse POT experiment is consistent with the measurement. On the other hand, the gain in the propeller efficiency of 2.32% for Propeller-A and 2.05% for Propeller-B at the condition close to the full scale condition is still smaller than the reported value of 4% in

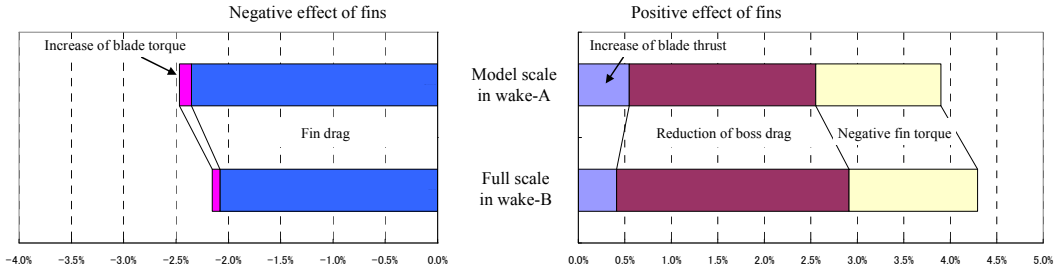

Figure 19 Comparison of the components of the effect of PBCF at J=0.7 for Propeller-A at model scale and full scale Reynolds numbers

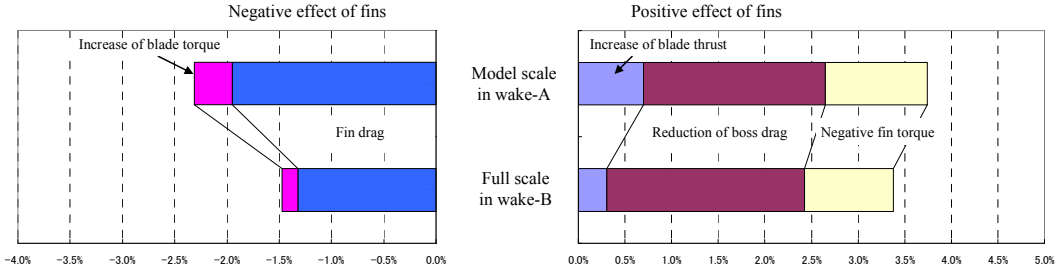

Figure 20 Comparison of the components of the effect of PBCF for Propeller-B at J=0.7 at model scale and full scale Reynolds numbers

the sea trial and logbook analysis. The reason for the remaining gap is not clear, but the difference in the estimated and actual wake distribution or other factors may be involved. Such factors which are not considered in this study include interaction with hull and rudder, surface roughness, unsteadiness, and hub vortex cavitation.

6 CONCLUSIONS

CFD computations were carried out in order to investigate the reasons for the difference in the effects of PBCF in model test and in full scale data. Computations were carried out for two different propellers at model and full scale Reynolds numbers with two different wake distributions. The results of the simulations corresponding to the reverse POT experiment were in a good agreement with the measurement. Computations at model scale and full scale Reynolds numbers with different wake distributions have shown that higher Reynolds number and the presence of wake of the hull positively influence the effect of PBCF. Due to the combined effect of the wake and the Reynolds number, the gain in the propeller efficiency for Propeller-A is increased from 1.48% at the condition corresponding to the reverse POT experiment to 2.32% at the condition close to the full scale condition, and that for Propeller-B is increased from 1.49% to 2.05%. The detailed investigation of the results suggested that the fin drag becomes smaller and the reduction of the boss drag becomes larger at the full scale condition.

However, the computed gain in the propeller efficiency, which is 2.32% for Propeller-A and 2.05% for Propeller-B, is still smaller than the reported value of 4% in the sea trial and logbook analysis. The remaining gap may be attributed to the difference in the estimated and actual wake distribution or to other factors such as interactions with hull and rudder, surface roughness, unsteadiness and hub vortex cavitation. Future studies considering such effects and more detailed measurement at full scale are expected to provide better understanding and better design of the device.

REFERENCES

Atlar M, Patience G (1998) An investigation into effective boss cap designs to eliminate propeller hub vortex cavitation. Proceedings of Practical Design of Ship and Mobile Units, Elsevier Science B.V., pp 757-769

Hansen H R, Dinham-Peren T, Nojiri T (2011) Model and Full Scale Evaluation of a 'Propeller Boss Cap Fins' Device Fitted to an Aframax Tanker. Second International Symposium on Marine Propulsors, smp'11, Hamburg, Germany

Hsin C-Y, Lin B-H, Chang C-H and Lin C-C (2008) The Analysis and Design of PBCF by Computation. Proceedings of the 4th Asia-Pacific Workshop on Marine Hydrodynamics APHydro 2008, Taipei

Kawamura T, Omori T, (2009) Reynolds Number Effect on Propeller Performance in Open Water. Journal of the Japan Society of Naval Architects and Ocean Engineers 10:29-36 (in Japanese)

Kawamura T, Watanabe T, Takekoshi Y, Maeda M, Yamaguchi H (2004) Numerical Simulation of Cavitating Flow around a Propeller. Journal of the Society of Naval Architects of Japan 195:211-219 (in Japanese)

Kawamura T (2011) Numerical Simulation of Propulsion and Cavitation Performance of Marine Propellers. Journal of JIME 46(3): 359-365

Nojiri T, Ishii N, Kai H (2011) Energy Saving Technology of PBCF (Propeller Boss Cap Fins) and its Evolution. Journal of JIME 46(3): 350-358

Ouchi K, Ogura M, Kono Y, Orito H, Shiotsu T, Tamashima M, Koizuka H (1988) A research and Development of PBCF (Propeller Boss Cap Fins) – Improvement of Flow from Propeller Boss -, Journal of Society of Naval Architects of Japan 163:66-78 (in Japanese)

Ouchi K, Tamashima M, Kawasaki T, Koizuka H (1989) A Research and Development of PBCF (Propeller Boss Cap Fins) : 2nd Report:Study on Propeller Slipstream and Actual Ship Performance. Journal of Society of Naval Architects of Japan 165:43-53 (in Japanese)

Ouchi K (1992) Effect and Application of PBCF (Propeller Boss Cap Fins). Journal of MESJ 27(9):768-778 (in Japanese)

Rhee S H, Kawamura T, Li H (2005) Propeller Cavitation Study Using an Unstructured Grid Based Navier-Stokes Solver. Journal of Fluids Engineering 127:986-994

The Specialist Committee on Unconventional Propulsors (1999) Final Report and Recommendations to the 22nd ITTC, pp 311-346

Yamasaki S (1989) Propeller Performance Characteristics in Ship Stern Flow Field : 1st Report : Effects of Ship Wake and Flow Contraction by Propeller, Transactions of the West Japan Society of Naval Architects (78), 101-111 (In Japanese)